



Separation of nickel and cobalt in aqueous solution by Ni²⁺-imprinted chitosan beads: behavior and mechanism

Na Guo, Wei-yi Sun, Bing Liao, Sang-lan Ding, Shi-jun Su*

Department of Environmental Science and Engineering, Sichuan University, Chengdu 610065, China

Tel./fax: +86 28 8546 0916; emails: sdzbg@126.com (Na Guo), swylscu@163.com (Wei-yi Sun), lben85@163.com (Bing Liao), dsjscu@163.com (Sang-lan Ding), ssjscu@163.com (Shi-jun Su)

Received 22 January 2016; Accepted 29 May 2016

ABSTRACT

Biosorbent Ni²⁺-imprinted chitosan beads were synthesized using epichlorohydrin cross-linking and nickel ion as the template for the selective adsorption of nickel ions from bimetallic aqueous solution comprising Ni²⁺ and Co²⁺. The effect of several parameters, i.e., pH, initial metal ions concentration, and contact time on the adsorption capacity and separation coefficient was examined. The selective and competitive adsorption processes of nickel and cobalt ions on the Ni²⁺-imprinted chitosan beads were studied separately. The equilibrium adsorption data of nickel could be well fitted with the Langmuir model even in the presence of high background cobalt concentrations, and the kinetics data were best fitted with the pseudo-second order kinetics model. In sole solution, the non-selective adsorption capacities of nickel and cobalt reached maximum (44.8 and 17.8 mg g⁻¹, respectively) at a solution pH of 5. In a binary metal species solution, when the cobalt-to-nickel concentration ratio was 1,500, the separation coefficient ($K_{Ni/Co}$) was ~45, indicating the excellent selectivity of the beads toward nickel adsorption. It was also found that initially adsorbed cobalt ions on Ni-imprinted chitosan beads were displaced by subsequently adsorbed nickel ions from the solution. It was speculated that the displacement result from an adjacent adsorption and repulsion mechanism. Additionally, Fourier transform infrared and X-ray photoelectron spectroscopy results revealed that the Ni²⁺-imprinting technology enabled the generation of abundant recognition sites for nickel ions on the Ni²⁺-imprinted chitosan beads and amine groups primarily bound to Ni²⁺ via chelation.

Keywords: Ni-imprinted chitosan; Separation coefficient; Nickel; Cobalt

1. Introduction

Cobalt and nickel typically co-exist in deposits [1], catalysts [2], batteries [3], Ni–Co alloys [4], and industrial waste solutions [5] owing to their similar physical and chemical properties. Consequently, to date, their separation in hydrometallurgy and recovery processes from secondary resources remains challenging. When compared with conventional separation processes, such as chemical precipitation [6], ion exchange [7], solvent extraction [8], and membrane separation technology [9], biosorption, which uses biological materials as adsorbents, has been considered as an innovative potential

technology for treating wastewater containing heavy metals owing to the economic viability and safe disposal of the spent adsorbent [10].

To our knowledge, numerous biosorbents have been studied in the field of adsorption [11–13]. Among them, chitosan and its derivatives are considered as promising biosorbents for the removal and recovery of metal ions from wastewaters because of their low cost, abundance in nature, environment-friendly properties, and high adsorption efficiency [14, 15]. Particularly, chitosan has great affinity for metal ions owing to the presence of abundant hydroxyl and amino groups on its backbone [16, 17]. However, the poor stability and selectivity of chitosan in aqueous acidic media limits its application in industrial effluents.

* Corresponding author.

To improve the chemical stability and mechanical strength of chitosan, cross-linking techniques employing different cross-linking agents have been widely used [12, 18]. However, the adsorption capacity of chitosan typically decreased after cross-linking due to the consumption of amine groups during cross-linking [19].

Ion-imprinted polymer (IIP) technology was introduced by Nishide et al. to improve adsorption selectivity by changing the template molecule into a metal ion based on the concept of molecularly imprinted polymers in 1976 [20]. In the last years, numerous studies relating to IIPs for the recognition of template ions, such as UO_2^{2+} [21], Cu^{2+} [22], Ni^{2+} [23], and Fe^{2+} [24], have been reported. Among these, novel bio-sorbent ion-imprinted chitosan resin has received much interest owing to its high selectivity and low cost. The merits of the cross-linking process and IIP technology have been exploited toward the preparation of ion-imprinted chitosan resins using metal ions as a template.

So far, ion-imprinted chitosan resins have been successfully applied in the selective adsorption of different metal ions such as Cu^{2+} [25], Co^{2+} [26, 27], Ag^{2+} [28], Ni^{2+} [29], UO_2^{2+} [30], and Pb^{2+} [31]. Research attention has been mostly focused on preparation and modification of the novel ion-imprinted chitosan-based biosorbent. However, few papers were designed to study the selective behaviors and mechanisms in detail, such as adsorption kinetic, adsorption isotherm and competitive adsorption process in the binary or multiple aqueous solutions. In fact, sole toxic metal species rarely exists in natural waste effluents. So a great effort should be made in research on the adsorption interaction on ion-imprinted chitosan resins involving two or more metal species, especially in the background of high metal ions concentration. And then the ion-imprinted chitosan resins could likely be applied to separate and recover certain metal ions from industry wastewater.

In the present study, Ni^{2+} -imprinted chitosan beads (denoted as Ni-IIP-CTS) were synthesized and investigated toward the adsorption interaction between nickel ions and cobalt ions in bimetallic solution. Great effort was devoted to examine the selective adsorption behavior of nickel ions on biosorbent in a binary metal ions system. Furthermore, displacement process and adsorption mechanisms were schematically elucidated.

2. Experimental

2.1. Materials and method

Chitosan >90% degree of deacetylation was obtained from Chengdu Kehua chemical factory (Sichuan, China). Nickel sulfate, Cobalt sulfate, acetic acid, epichlorohydrin (ECH), sodium hydroxide, ethylene diamine tetra-acetic acid (EDTA) and sulfate acid were purchased from Chuanxi Chemical factory (Sichuan, China) and used without further purification. Distilled water was used for preparation of metal stock solution. The desired pH-values were adjusted by dilute sodium hydroxide or sulfuric acid.

2.2. Preparation of the Ni^{2+} -imprinted chitosan beads

Ni^{2+} -imprinted chitosan beads (denoted as Ni-IIP-CTS) were synthesized in four major steps according

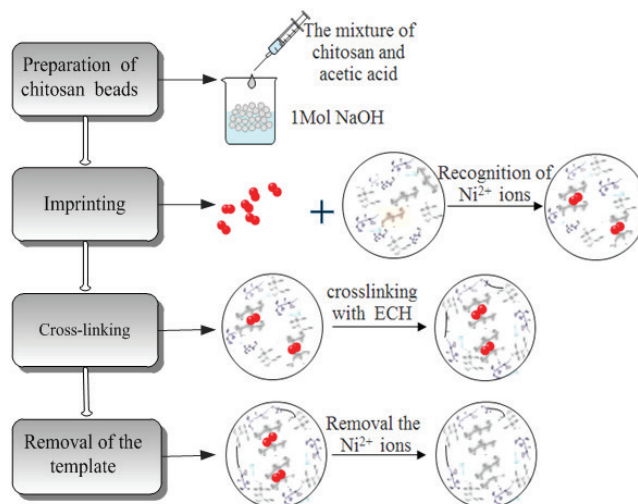


Fig. 1. Schematic procedure of the synthesis of Ni-IIP-CTS beads.

to the reported literature procedure [26, 29] with some modification (Fig. 1).

2.2.1. Preparation of chitosan beads

Chitosan (1 g) was dissolved in acetic acid solution (30 mL, 2%, v/v) while stirring using a magnetic stirrer to obtain a homogeneous chitosan. The gel mixture was then introduced dropwise into NaOH solution (100 mL, 1 M) with a syringe. The prepared chitosan beads were retrieved by filtration and rinsed with deionized water.

2.2.2. Adsorption of nickel template ions

Chitosan beads (10 g) were introduced into a nickel sulfate solution (50 mL, 10000 ppm) and shaken at 120 rpm for 24 h. The resulting nickel-loaded chitosan beads were retrieved by filtration and washed with deionized water.

2.2.3. Cross-linking with epichlorohydrin

Epichlorohydrin (10 mL) was introduced into a flask containing the nickel-loaded chitosan beads (10 g), and the cross-linking reaction proceeded for 24 h with shaking at 120 rpm and 333 K. The synthesized cross-linked chitosan beads were retrieved by filtration and washed sequentially with ethanol and deionized water.

2.2.4. Removal of nickel template ions

The nickel template ions were removed from the synthesized chitosan beads by extraction with 1 M sulfate acid solution and subsequently washed with deionized water. Then, these beads were treated with 1 M sodium hydroxide solution to regenerate the binding sites. Finally, the beads were washed with pure water for several times until the pH of the rinsing solution was neutral and stored until use.

The same process of preparation was carried out without adsorption of nickel template ions, and the obtained composites were non-imprinted chitosan beads, labeled as NIP-CTS.

2.3. Batch adsorption study

All batch adsorption experiments were conducted at 313 K and constant shaking at 120 rpm. The adsorbent-to-solution ratio was 1 g L⁻¹. For comparison, the adsorption studies of nickel were conducted in both the single and binary metal species systems with Ni-IIP-CTS and NIP-CTS, respectively.

2.3.1. Effect of pH

The effect of pH on the adsorption property of nickel was investigated in the pH range of 2–6. Portions (0.05 g) of biosorbent (Ni-IIP-CTS or NIP-CTS) were introduced into respective 250-mL conical flasks containing the metal solution (50 mL). In the single metal species system, the initial concentration of metal ions was 20 ppm. For the binary metal species system, the initial concentration of nickel was 20 ppm and the concentration of cobalt ions was either 200 or 1,000 ppm. The beads and metal solution-containing conical flasks were shaken for 24 h, and the final concentration of the metal ions was determined.

2.3.2. Adsorption isotherm studies

Adsorption isotherms were obtained for the single and binary metal species systems at the optimum pH of 5. Biosorbent (0.05 g) were introduced into a 250-mL conical flask comprising the metal solution (50 mL). The concentration of nickel was varied in the range of 20–100 ppm and that of the cobalt ions was varied in the range of 0–1,000 ppm. The beads and metal solution-containing conical flasks were shaken for 24 h, and the final concentration of the metal ions was determined.

2.3.3. Adsorption kinetics studies

The adsorption kinetics studies of nickel on biosorbent in the single and binary metal species systems were conducted in a 2-L flask containing adsorbent (1,000 g) and metal solution (1,000 mL) at pH 5, respectively. In the single metal species system, the initial concentration of nickel was 20 ppm. In the binary metal species system, the initial concentration of nickel was fixed at 20 ppm and that of cobalt was varied in the range of 0–3,500 ppm. Aliquots (1 mL) were withdrawn at regular intervals to determine the concentration of the metal ions.

2.3.4. Metal ions displacement studies

A displacement test was additionally conducted to investigate the possible displacement of initially adsorbed metal ions by subsequently adsorbed metal ions. In the first experiment, Ni-IIP-CTS (1 g) were first introduced into a nickel ions solution (1,000 mL) with an initial nickel ion concentration of 100 ppm and left to be shaken for 24 h. The nickel-loaded beads (denoted as Ni-loaded) were separated through filtration. The resulting beads (0.5 g) were then introduced into (a) a cobalt ions solution (500 mL) with an initial cobalt ions concentration of 100 ppm (the resulting beads are referred as Ni–Co-loaded) and (b) deionized water (500 mL) at pH 5 as a blank experiment (the resulting beads are referred as Ni–W-loaded) and left to be shaken for 24 h. Aliquots were

withdrawn to monitor changes in the metal ions concentration in the solution as a function of contact time.

A similar second experiment was conducted, however, the beads were loaded with cobalt first (denoted as Co-loaded) and subsequently loaded with nickel or water (as a blank experiment) under the same conditions (bead amount, pH, and volume and concentration of metal ions solution) used above. The beads are referred as Co–Ni-loaded and Co–W-loaded, respectively.

2.4. Analytical methods

2.4.1. Characterization methods

The metal ions concentration was measured by an ICP-MS (NEXION 300X, PE) equipped with an auto-sampler (SC2 DX, ESI). The Fourier-Transform Infrared Spectroscopy (FTIR6700, Nicolet, USA) was used to characterize the chemical bonds of Ni-IIP-CTS beads before and after metal adsorption. All samples of FTIR spectrometer were prepared by KBr pellets and scanned in the range 4,000 to 400 cm⁻¹. X-ray photoelectron spectroscopy (XPS, XSAM-800, KRATOS, UK) was used to characterize the states of the certain elements on the surface of Ni-IIP-CTS beads with or without metal ion load. The XPS analysis was obtained with an Al K α X-ray source (1486.6 eV of protons).

2.4.2. Data processing

The equilibrium adsorption capacity (q_e /mg g⁻¹), amount of distribution ratio K_d [32] and separation coefficient of Ni²⁺ over Co²⁺ ($K_{Ni/Co}$) [33] was calculated by the following equation.

$$q_e = \frac{(c_0 - c_e) \cdot V}{m} \quad (1)$$

$$K_d = \frac{(C_0 - C_e)}{C_e} \times \frac{V}{m} \quad (2)$$

$$K_{Ni/Co} = \frac{K'_d(Ni)}{K'_d(Co)} \quad (3)$$

where C_0 and C_e are the initial and equilibrium metal concentration (mg/g), m is the mass of adsorbent (g) and V is the volume of solution (L), K_d is the distribution ratio in binary system.

3. Results and discussion

3.1. Effect of initial pH-value on selective adsorption

The solution pH plays a key role on the adsorption capacity of metal ions owing to its effect on the generation of varied metal ion forms [34]. Fig. 2 showed the adsorption behavior of biosorbent toward nickel and cobalt ions at varying pH-value in sole metal ions system. In Fig. 2(a), the adsorption capacity of nickel ions and cobalt ions on NIP-CTS increased remarkably with the increasing of pH at pH less than 4. The higher adsorption capacities observed with increasing pH-value was attributed to the reduced formation of protonated amine groups at increasing pH-value, which otherwise

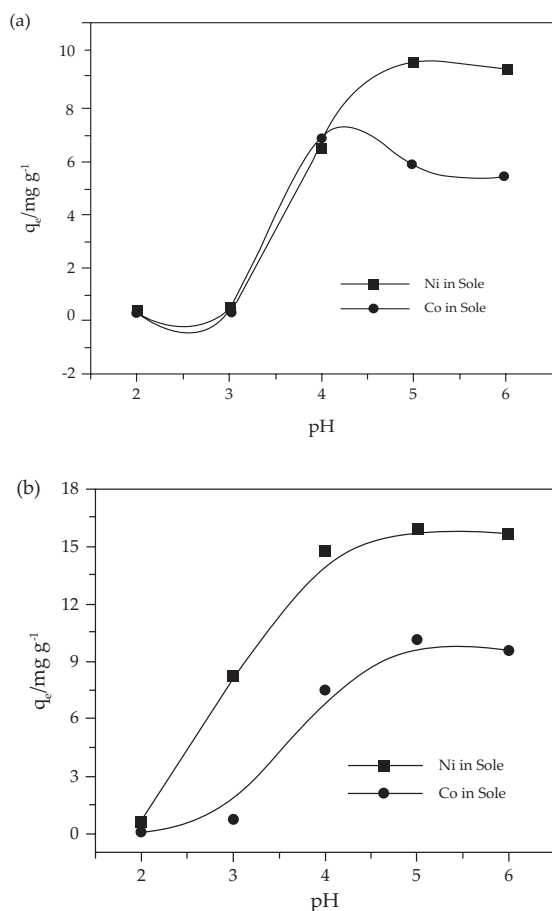


Fig. 2. Effect of pH-value on adsorption capacity of nickel and cobalt in sole solution onto (a) NIP-CTS and (b) Ni-IIP-CTS.

inhibited the adsorption of metal ions. The maximum adsorption values for nickel ions and cobalt ions onto NIP-CTS were 8.89 and 6.67 mg g^{-1} at around pH = 5 and pH = 4 respectively, from which the separation adsorption of nickel over cobalt on NIP-CTS was hardly observed. Similar nickel and cobalt adsorption behaviors were observed in Fig. 2(b), and corresponding maximum adsorption capacities of 15.65 and 8.7 mg g^{-1} were obtained at pH 5, which were higher than that on NIP-CTS. Moreover, the adsorption capacity of nickel on Ni-IIP-CTS was higher than that of cobalt regardless of the solution pH-value, thus indicating the adsorption preference behavior of Ni-IIP-CTS toward nickel ions. In addition, the Ni-IIP-CTS show greater pH-value adaptability than that of NIP-CTS.

To effectively determine the separation efficiency of nickel ions in the presence of competitor species cobalt, the separation coefficient, $K_{\text{Ni/Co}}$ was determined. The effect of pH on $K_{\text{Ni/Co}}$ in the binary metal species system was shown in Fig. 3. Parameter $K_{\text{Ni/Co}}$ changed considerably with changes in pH in the range of 2–6. Maximum separation coefficient $K_{\text{Ni/Co}}$ was achieved at pH 3 in both binary metal species systems studied (where the Co-to-Ni concentration ratios = 50 and 10). Based on the results obtained, a pH value of 5 was selected as the optimum to achieve both high adsorption capacity and separation coefficient; moreover, such a pH was suitable for

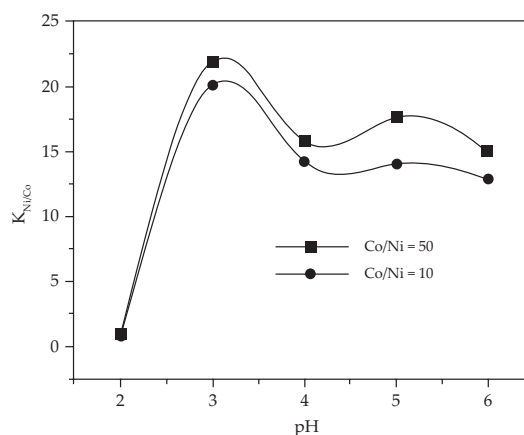


Fig. 3. Effect of pH-value on separation coefficient of Ni²⁺ over Co²⁺ in binary system onto Ni-IIP-CTS.

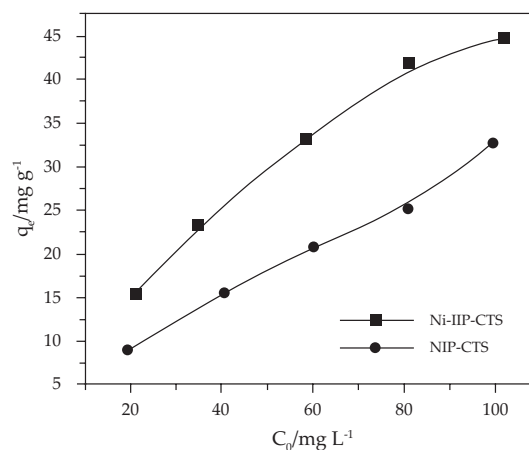


Fig. 4. Effect of initial concentration of metal ions on the adsorption capacity of nickel on biosorbent in sole nickel solution.

practical application. Hence, subsequent experiments were conducted at pH 5. When the initial cobalt-to-nickel concentration ratio was 10 (denoted as Co/Ni = 10), $K_{\text{Ni/Co}}$ was lower than that obtained at Co/Ni = 50, thus confirming the high selectivity of Ni-IIP-CTS toward nickel adsorption in the presence of high background cobalt concentrations. The reason for such a result will be discussed in Section 3.4.

3.2. Adsorption isotherm studies

Fig. 4 showed the effect of the initial metal ion concentration on the nickel adsorption capacity of Ni-IIP-CTS and NIP-CTS in the single metal species system. As observed from Fig. 4, in the range of studied concentration, the equilibrium adsorption capacity of nickel ions all increased with increasing initial nickel concentrations. Furthermore, it could be found that the adsorption capacity of Ni-IIP-CTS was greater than that of NIP-CTS at the identical initial concentration of nickel, confirming the effect of IIP technology.

The adsorption isotherm of nickel ions on Ni-IIP-CTS in binary system were presented in Fig. 5. A similar nickel adsorption capacity profile with Ni-IIP-CTS was observed in

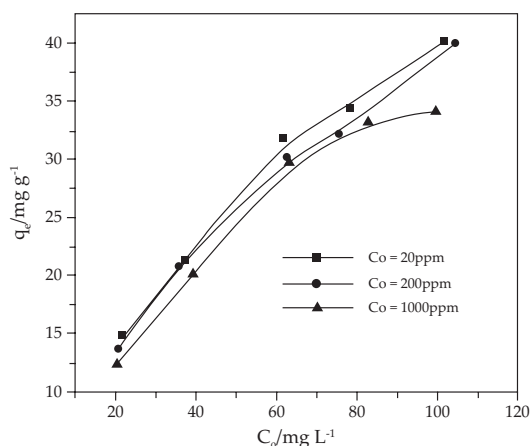


Fig. 5. Effect of initial concentration of metal ions on the adsorption capacity of nickel on Ni-IIP-CTS in binary system.

Fig. 5 (wherein the initial concentration of cobalt was fixed) with increasing initial nickel concentrations. However, the equilibrium adsorption capacity of nickel ions decreased when the initial concentration of cobalt increased, while that of nickel was kept constant. This result was attributed to the onset of competitive adsorption of cobalt on the binding sites of the beads. In the binary metal species system, when the initial nickel concentration was 20 ppm, the equilibrium adsorption capacity of nickel decreased from 14.88 to 12.27 mg g⁻¹ (corresponding to a decrease of 17.50%) with increasing initial cobalt concentrations from 20 to 1,000 ppm. This result demonstrated the excellent competitive adsorption of Ni-IIP-CTS for nickel over cobalt.

In present work, all the nickel adsorption isotherm data were analyzed with the Langmuir models and Freundlich models as described by Eqs. (4) and (5), respectively. The associated calculated adsorption parameters are listed in Table 1.

Langmuir model:

$$\frac{1}{q_e} = \frac{1}{q_\infty} + \frac{1}{q_\infty K_L c_e} \tag{4}$$

Freundlich model:

$$\ln q_e = \frac{1}{n} \ln c_e + \ln K_f \tag{5}$$

Table 1
Isotherm model constants for the adsorption of nickel at different concentration of nickel and cobalt

Adsorbent	Solution system	Experimental	Langmuir			Freundlich		
		q_e	Q_{max} mg g ⁻¹	K_L mg L ⁻¹	R^2	K_f	$1/n$	R^2
NIP-CTS	Ni in sole	32.70	46.25	0.0235	0.9727	1.9011	0.6637	0.9945
Ni-IIP-CTS	Ni in sole	44.84	53.19	0.0760	0.9956	7.7459	0.4446	0.9815
	Co = 20 ppm	40.18	49.18	0.0564	0.9883	5.7863	0.4786	0.9851
	Co = 200 ppm	40.08	47.52	0.0572	0.9944	5.6724	0.4739	0.9838
	Co = 1000 ppm	34.17	46.72	0.0442	0.9905	4.4734	0.5065	0.9617

where K_L is the Langmuir sorption constant (L/mg) and reflects the free energy of sorption, q_∞ is the most adsorption capacity, K_f and n are the parameters of Freundlich isotherm and related to the activity of adsorption.

As presented in Table 1, the adsorption process on NIP-CTS was better described by the Freundlich model than the Langmuir model, thereby indicating that the adsorption of nickel on the biosorbent was multilayer adsorption. However, the Langmuir model could relatively better predict the isotherm data of nickel ions onto Ni-IIP-CTS in both systems. So the adsorption of nickel ions on Ni-IIP-CTS belonged to monolayer adsorption. Furthermore, the maximal adsorption capacity of biosorbent calculated via Langmuir model at each case were all closed to experimental values. Parameters K_L and $1/n$, associated with the Langmuir and Freundlich models, respectively, ranged between 0 and 1 for the different initial concentration ratios studied, thereby indicating that Ni-IIP-CTS and NIP-CTS were an ideal adsorbent for nickel ions removal. However, the greater Q_{max} of Ni-IIP-CTS compared with that of NIP-CTS implies that Ni-IIP-CTS showed the greater affinity than NIP-CTS due to the ion-imprinting technology during preparation process.

Comparison of the adsorption performance of Ni²⁺-imprinted chitosan with other adsorbents for Ni²⁺ ion, such as common adsorbents, reported in the literatures were shown in Table 2. As presented in Table 2, the adsorption capacity of Ni-IIP-CTS was higher than most of the reported sorbent [18, 35, 36, 37] and lower than some of those published adsorbent [29, 38, 39]. Most of the reported adsorbent were absence of the selectivity coefficient ($K_{Ni/M}$) [18, 35–37, 39]. The selectivity coefficient $K_{Ni/Co}$ of Ni-IIP-CTS was higher than the Ni-imprinted magnetic chitosan/PVA adsorbent [29] and lower than the NDC-984 resin [38]. However, the high selective coefficient of NDC-984 resin was obtained with a high initial concentration ratio of 5000. So the comparison confirmed that the Ni-IIP-CTS had certain application prospect for selective nickel remove.

3.3. Adsorption kinetics studies

The adsorption kinetics results of nickel on both biosorbent in sole solution were presented in Fig. 6. It should be noted that the adsorption capacity increased with increasing contact time and the adsorption equilibrium reached within 8 h and 6 h on Ni-IIP-CTS and NIP-CTS, respectively. Furthermore, the adsorption capacity of Ni-IIP-CTS was greater than that of NIP-CTS, clearly indicating the imprinting effect on adsorption capacity.

Table 2
Comparison of different adsorbent for nickel ion

Adsorbent	$Q_{\max} / \text{mg.g}^{-1}$	T/K	pH	Isotherm	Kinetic	$K_{\text{Ni/M}}$	Refs.
Chitosan encapsulated Sargassum sp.	19.85	298	7	Freundlich	Pseudo Second-order	–	[35]
Ni-imprinted magnetic chitosan /PVA	500	298	5–6	Langmuir	Pseudo Second-order	$K_{\text{Ni/Ag}} = 23;$ $K_{\text{Ni/Cu}} = 15;$ $K_{\text{Ni/Zn}} = 18$	[29]
γ -alumina nano-particles	49.7	313	6	Langmuir-Freundlich	Pseudo Second-order	–	[36]
NDC-984 resin	66.1	303	5	Langmuir	Pseudo Second-order	$K_{\text{Ni/Co}} = 80$	[38]
Carboxylated sugarcane bagasse	91.9	298	5.75	Slip	Pseudo Second-order	–	[39]
Polyurethane foam	24.39	313	5.5	Freundlich	Pseudo Second-order	–	[37]
GLA - crosslinked Ni^{2+} imprinted chitosan	37.88	298	5	Langmuir	Pseudo Second-order	–	[18]
Ni-IIP-CTS	53.19	5	313	Langmuir	Pseudo Second-order	$K_{\text{Ni/Co}} = 45$	In this work

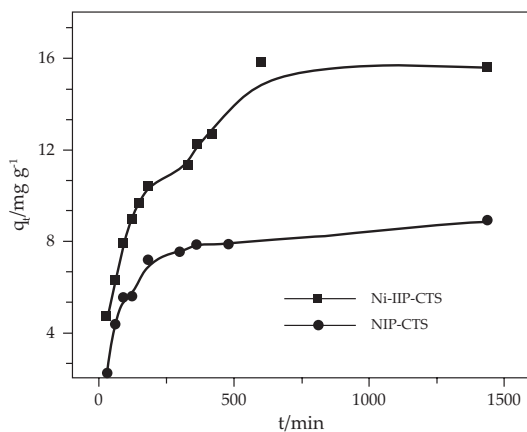


Fig. 6. Effect of contact time on adsorption kinetics of nickel with Ni-IIP-CTS and NIP-CTS in sole solution.

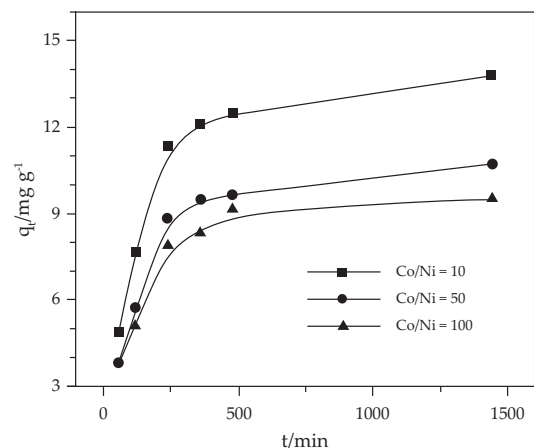


Fig. 7. Effect of contact time on adsorption kinetics of nickel with Ni-IIP-CTS in binary system.

Fig. 7 showed the competitive adsorption kinetics of nickel on Ni-IIP-CTS in binary system. In Fig. 7, it is observed that nickel ions adsorption on Ni-IIP-CTS had similar performance to that in the sole solution (Fig. 6). However, the uptake capacity decreased with increasing initial cobalt concentrations, as consistent with the results in Fig. 5, thus demonstrating the competitive adsorption between cobalt ions and nickel ions.

To further evaluate the adsorption process, several adsorption kinetic models, such as the pseudo-first-order equation, pseudo-second-order equation, intraparticle diffusion model, and Elovich rate equation, can be used. Among them, the pseudo-first-order and pseudo-second-order equations are mainly employed in biosorption. Hence, the obtained adsorption kinetics data were fitted with both the

pseudo-first-order and pseudo-second-order equations. The associated determined parameters were presented in Table 3. As observed, the calculated correlation coefficient (R^2) values of the pseudo-second-order-kinetics-model-fitted data were higher than those of the pseudo-first-order-kinetics-model-fitted data. Accordingly, it could be deduced that the adsorption of nickel on the both biosorbents were better described by the pseudo-second-order kinetic model, which implied that the chemical interaction between the metal ions and ligands was the rate-limiting step of the adsorption process. Furthermore, the equilibrium adsorption capacity q_e of nickel obtained by modeling was comparable to the experimentally obtained capacity in each case studied. The rate constant k_2 is an indicator of the inhibition effect exerted by interfering ions—the lower the k_2 value, the greater the inhibition

Table 3
Kinetic model constants for the adsorption of nickel at different concentration of nickel and cobalt

Biosorbent	Solution system	Experimental q_e	Pseudo-first-order			Pseudo-second-order		
			q_e	k_1	R^2	q_e	k_2	R^2
NIP-CTS	Ni in sole	8.89	10.80	0.0092	0.9703	9.21	0.001774	0.9964
Ni-IIP-CTS	Ni in sole	15.63	14.43	0.0033	0.9513	16.83	0.000552	0.9937
	Co/Ni=10	13.80	13.33	0.0074	0.9860	14.79	0.000703	0.9987
	Co/Ni=50	10.72	10.41	0.0071	0.9834	11.53	0.000873	0.9983
	Co/Ni=100	9.49	9.34	0.0073	0.9745	10.14	0.000881	0.9977

effect is. As observed in Table 2, in binary system studied, k_2 increased with increasing initial molar ratios, thereby indicating that the inhibition effect exerted by cobalt ions on the adsorption of nickel ions onto Ni-IIP-CTS decreased. As a result, it was easier to selectively extract nickel ions from a higher Co-to-Ni concentration ratio solution and realize the separation of nickel and cobalt by Ni-IIP-CTS.

Pseudo first-order kinetics:

$$q_t = q_e(1 - e^{-k_1 t}) \quad (6)$$

$$\log(q_e - q_t) = \log(q_e) - \frac{k_1}{2.303} t \quad (7)$$

Second-order kinetic equation:

$$q_t = \frac{q_e^2 k_2 t}{1 + q_e k_2 t} \quad (8)$$

$$\frac{t}{q_t} = \frac{1}{k_2 q_e^2} + \frac{t}{q_e} \quad (9)$$

where q_e and q_t are the adsorption capacity (mg/g) at equilibrium and at time t (min), respectively; and k_1 (min^{-1}) is the rate constants of pseudo-first order kinetic model; k_2 ($\text{g} \cdot \text{mg}^{-1} \cdot \text{min}^{-1}$) is the rate constants of second-order kinetic model.

3.4. Competitive and selective adsorption studies

Fig. 8 showed the adsorption kinetics of nickel and cobalt on Ni-IIP-CTS (Figs. 8(a)–(b)) and NIP-CTS (Figs. 8(c) and (d)) in the single and binary metal species systems, the initial concentration of both metal ions was 20 ppm in both systems, respectively. Comparison of the data shown in Figs. 8(a) and 8(b) revealed that the adsorption of nickel on Ni-IIP-CTS was efficient in both the single and binary metal species systems. In contrast, the adsorption of cobalt ions on Ni-IIP-CTS was greatly depressed in the presence of co-existing nickel ions in solution. Specifically, adsorption of the cobalt ions was observed in the first 180 min of the process, however, subsequently decreased under prolonged contact times. Thus, contact time is an important factor to consider in the separation of nickel and cobalt in aqueous

solution using Ni-IIP-CTS. It was deduced that the cobalt ions initially adsorbed on Ni-IIP-CTS were subsequently released from the adsorbent into the solution.

Fig. 8(c) and 8(d) showed the adsorption performance in sole solution was similar to that on Ni-IIP-CTS, but that in binary system was obviously different. The decline range of adsorption capacity for nickel ions was similar to that for cobalt ions in binary system, indicating that NIP-CTS showed poor selective adsorption for nickel ions toward cobalt ions.

Thus, the results in Fig. 8 clearly demonstrated the stronger competitive and selective adsorption behavior of nickel ions over cobalt ions on Ni-IIP-CTS than that on NIP-CTS due to the imprinting effect. As a result, nickel ions were selectively adsorbed and separated from cobalt ions in the binary metal species system. Furthermore, the test outcomes prove further the imprinting effect on selectivity of biosorbent.

Fig. 9 showed the effect of the Co-to-Ni concentration ratio (denoted as Co/Ni) on the distribution coefficient K_d and separation coefficient $K_{\text{Ni/Co}}$. At a given initial nickel concentration, K_d values of the two metal species decreased with increasing initial concentration ratios owing to the competitive reaction. However, the K_d values of cobalt ions declined more rapidly than those of nickel. Thus, the separation efficiency of nickel (from cobalt) increased considerably, implying that the selective adsorption of nickel on Ni-IIP-CTS was excellent. The $K_{\text{Ni/Co}}$ results were consistent with the k_2 results in Table 3. Consequently, the results in Table 3 combined with that in Fig. 9 clearly demonstrated the high selective adsorption behavior of nickel ions on Ni-IIP-CTS, even in the presence of high background cobalt concentrations. This result agreed with the findings reported by Bhaskarapillai et al., confirming that the ion-imprinted technology can selectively recognize template ions in a complex mixture of metal ions though the ion radii and charge-to-radius ratios of the metal ions are similar [40].

3.5. Displacement of cobalt and nickel on Ni-IIP-CTS

To determine whether metal ions initially adsorbed on Ni-IIP-CTS can be displaced by different subsequently adsorbed metal ions, a series of experiments were performed, and the results were shown in Fig. 10. Figs. 10(a) – (b) showed the kinetic results of Ni-IIP-CTS, already loaded with 17.84 mg g^{-1} cobalt ions (denoted as Co-loaded), was placed in a nickel ion solution with an initial concentration

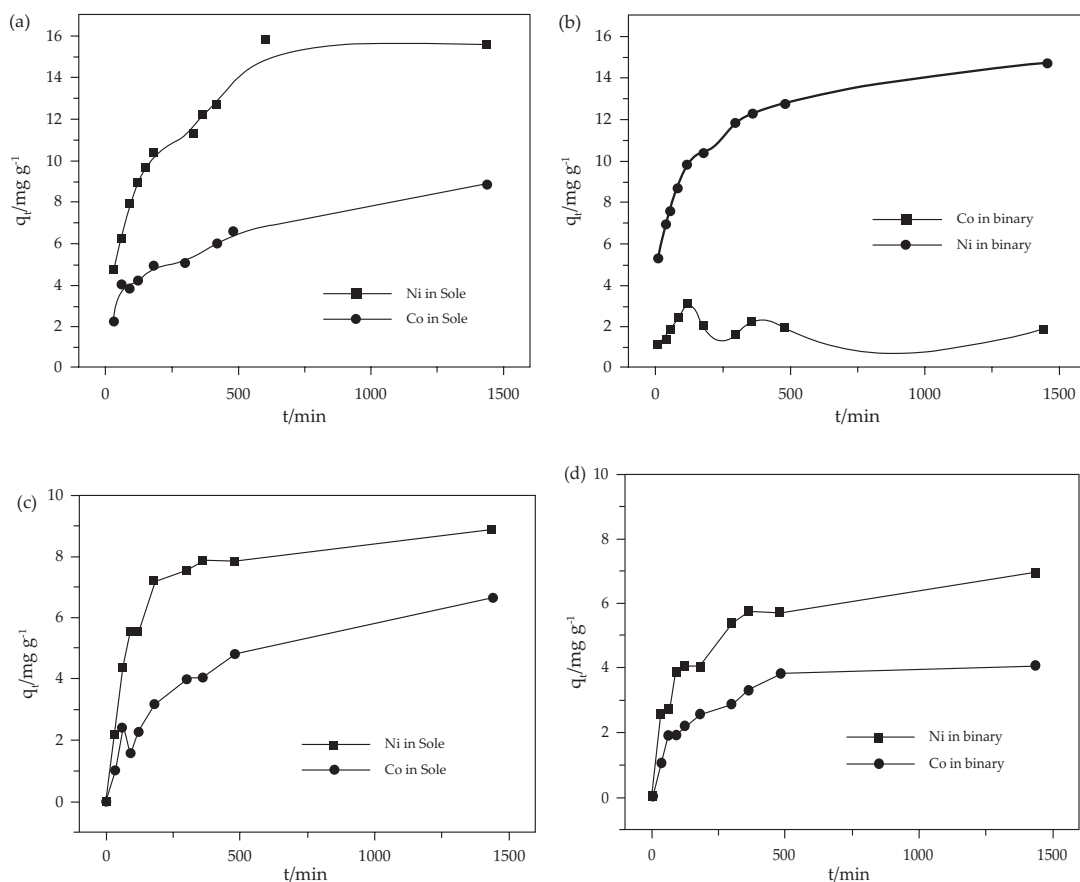


Fig. 8. Adsorption kinetics curve of nickel and cobalt ions on Ni-IIP-CTS ((a), (b)) and NIP-CTS ((c), (d)) in sole solution and in binary system.

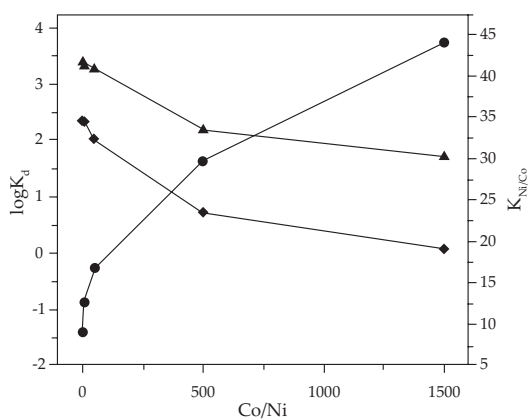


Fig. 9. Distribution coefficient (K_d) and separation coefficient ($K_{Ni/Co}$) for nickel and cobalt with different initial concentrations ratio.

of 100 ppm (denoted as Co-Ni-loaded in Fig. 10(a)) or in DI water (denoted as Co-W-loaded in Fig. 10(b)). From Fig. 10(a), the amount of cobalt ions released from the biosorbent into the solution was 14.2 mg g^{-1} (corresponding to $\sim 79.6\%$), and the amount of nickel subsequently adsorbed onto Ni-IIP-CTS from solution was 27.7 mg g^{-1} . From the result

presented in Fig. 10(a), it was interesting to find that the amount of Ni-adsorption on Co-loaded was higher than that of Co-released from Co-loaded biosorbent, indicating the presence of abundant special active sites for selective adsorption nickel ions from the complex mixture of metal ions in solution owing to the template matrix in Ni-IIP-CTS. In the blank experiment Fig. 10(b), only 7.0 mg g^{-1} (corresponding to $\sim 39.2\%$) of adsorbed cobalt ions was released in to DI water from Co-loaded. These results in Fig. 10(c) showed that the previously adsorbed cobalt ions were indeed displaced (about 40.4%) by the subsequent adsorption of nickel ions.

Similar kinetics results on the behaviors of Ni-loaded in cobalt ions solution with an initial concentration of 100 ppm (denoted as Ni-Co-loaded) or DI water (denoted as Ni-W-loaded) were shown in Fig. 10(d) and (e) respectively. As observed in Fig. 10(d), only 3.2 mg g^{-1} of cobalt ions was adsorbed onto the biosorbent from the solution. And the amount of nickel ions released from Ni-IIP-CTS upon subsequent adsorption of cobalt ions was 16.5 mg g^{-1} (corresponding to $\sim 37\%$). However, in blank experiment Fig. 10(e) about 14.0 mg g^{-1} (corresponding to $\sim 31\%$) adsorbed nickel ions was released into DI water. The results shown in Fig. 10(f) indicated that adsorbed nickel ions on Ni-imprinted were barely displaced (only about 6%) by the subsequent adsorption of cobalt ions on the biosorbent.

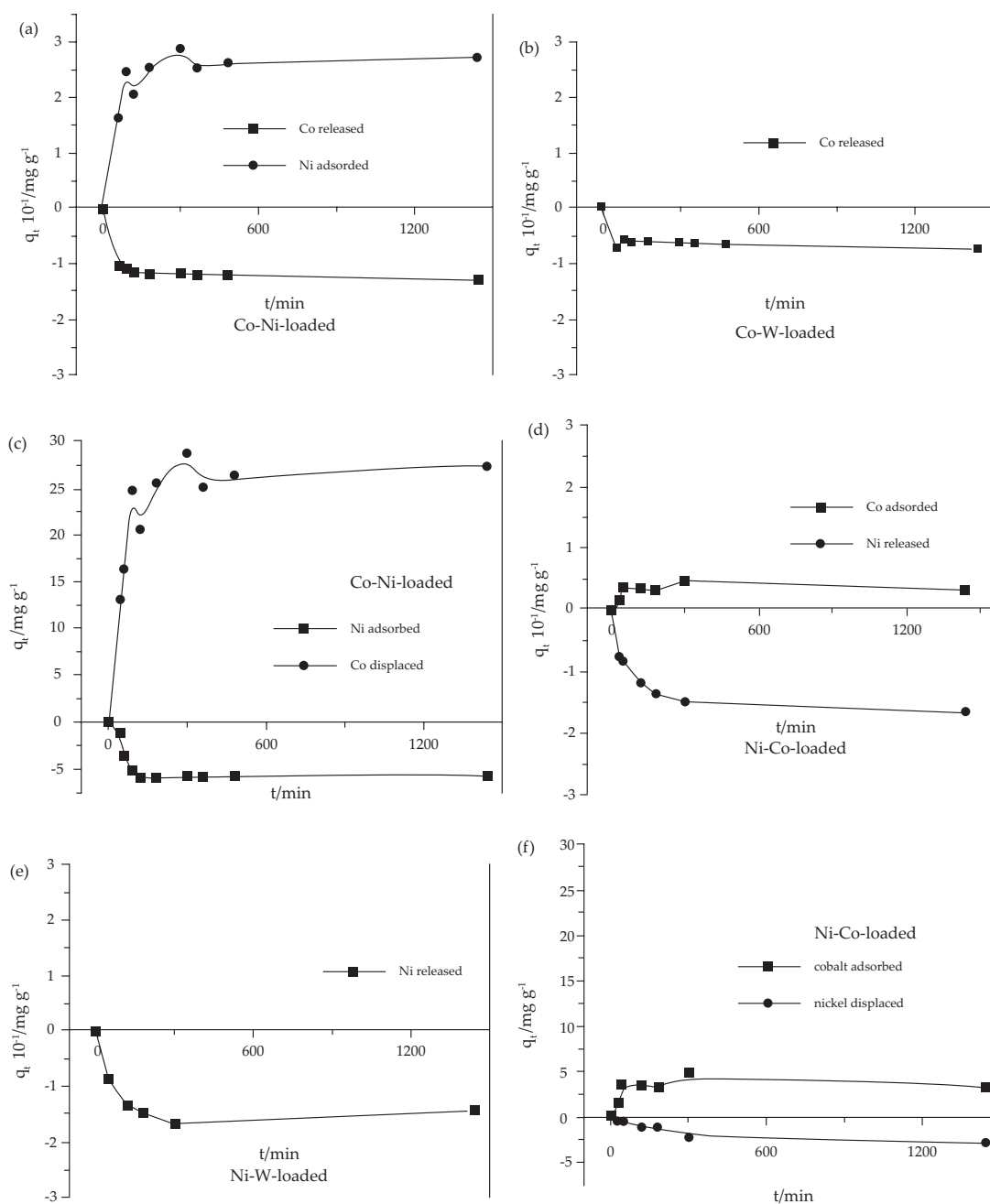


Fig. 10. Cobalt and nickel ions displacement adsorption kinetics on the biosorbent.

3.6. Determination of the adsorption mechanism

To elucidate the adsorption mechanism further, the surface interactions involved in the adsorption process were examined.

3.6.1. FTIR spectroscopy studies

The FTIR spectra of Ni-IIP-CTS before and after metal ions adsorption were shown in Fig. 11. Fig. 11(a) showed the characteristic peaks of the Ni-imprinted chitosan

beads at 3430 cm^{-1} (corresponding to O–H and N–H stretches, overlap), 2923 and 2880 cm^{-1} (corresponding to C–H stretch), 1650 and 1560 cm^{-1} (corresponding to N–H stretch), 1155 cm^{-1} (corresponding to $\text{C}_3\text{-OH}$) and 1031 cm^{-1} (corresponding to $\text{C}_6\text{-OH}$) [28, 41]. In contrast, the peaks corresponding to –OH and –NH groups originally observed at 3430 cm^{-1} shifted to 3425 cm^{-1} (Fig. 11(c)) and 3411 cm^{-1} (Fig. 11(b)) after nickel and cobalt uptake, respectively. Additionally, the peaks corresponding to $\text{C}_3\text{-OH}$, $\text{C}_6\text{-OH}$, and –NH were weaker.

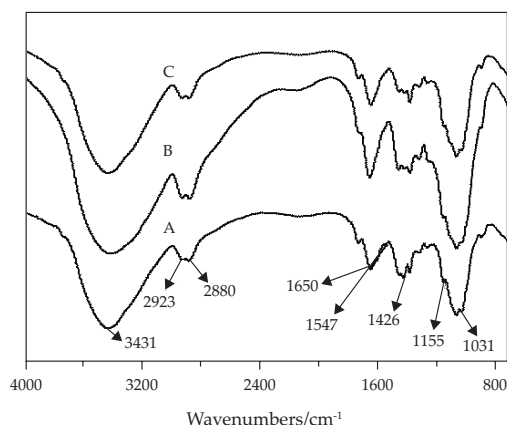


Fig. 11. FTIR spectra of (a) Ni-IIP-CTS beads, (b) cobalt-loaded Ni-IIP-CTS beads, (c) nickel-loaded Ni-IIP-CTS beads.

The changes observed after metal uptake implied that the functional groups i.e., N–H and O–H are involved in the adsorption process.

3.6.2. XPS studies

XPS was used to further investigate the adsorption mechanism. As shown in the wide XPS scans in Figs. 12(a)–(c), characteristic peaks of carbon atom (C 1s), oxygen atom (O 1s), and nitrogen atom (N 1s) were observed for Ni-IIP-CTS, and peaks of nickel atom (Ni 2p) or cobalt atom (Co 2p) were additionally observed for the Ni-loaded or Co-loaded biosorbent, respectively. These results confirmed that nickel or cobalt ions were adsorbed on the biosorbent.

Furthermore, elemental (O 1s and N 1s) XPS analyses of the biosorbent before and after metal uptake were performed, and the results were shown in Figs. 12(a)–(c). Comparison of the XPS spectra obtained before and after metal adsorption revealed that the binding energies of N and O elements changed obviously after nickel uptake and cobalt adsorption, respectively.

The N 1s spectra of Ni-IIP-CTS comprised two peaks with different binding energies, as shown in Fig. 13. The peaks at 398.76 and 399.85 eV were attributed to N–H₃⁺, and –NH– and NH₂, respectively [35, 37]. After the adsorption of nickel on the biosorbent, the binding energies of the peaks corresponding to N–H₃⁺, and –NH– and –NH₂, respectively increased to 399.05 and 401.10 [42], and 400.00 eV. The appearance of peak at a binding energy of ~400.0 eV could be due to the nitrogen coordinated with a heavy metal ions (i.e., R–NH₂Ni), in which a lone pair of electrons from the N atom are shared between N and nickel ions. Consequently, the electron cloud density of N atom become small, thus leading to a higher binding energy peak [35]. Thus, the N 1s XPS spectrum of the biosorbent after nickel uptake confirmed that chelation between the amine groups of the biosorbent and Ni²⁺ ions was one of adsorption mechanisms. In contrast, the binding energy of the peak corresponding to N 1s barely changed after cobalt adsorption, thereby indicating that N-containing groups showed negligible affinity for cobalt for adsorption on Ni-IIP-CTS.

Fig. 13(a)–(c) additionally showed that the binding energies of the O 1s bands in Ni-IIP-CTS increased from 531.12 and

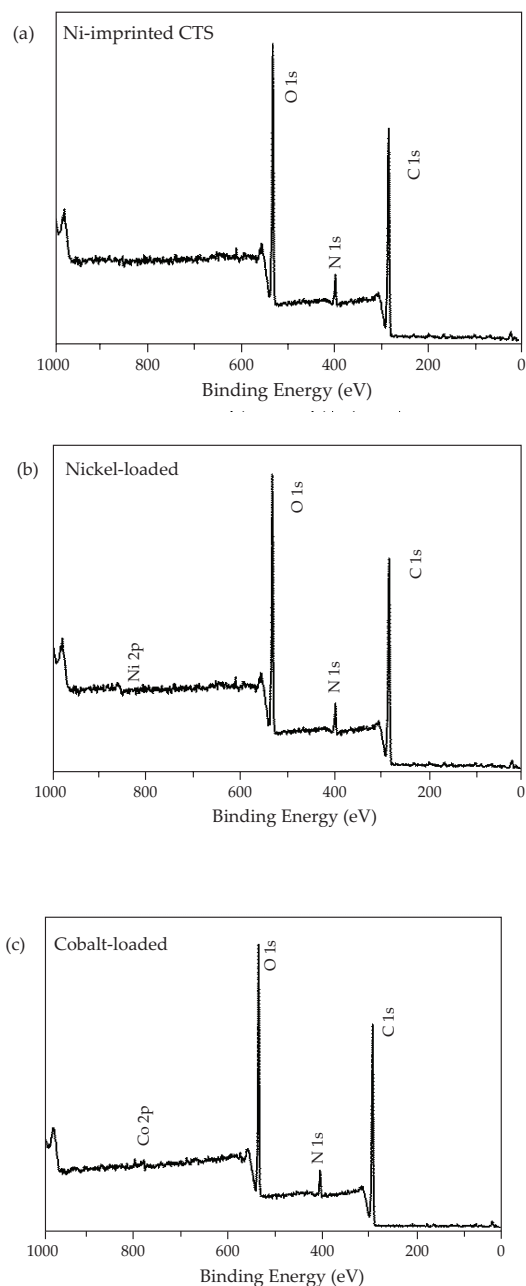


Fig. 12. Wide-scan XPS spectra of (a) Ni-IIP-CTS beads, (b) nickel-loaded Ni-IIP-CTS beads and (c) cobalt-loaded Ni-IIP-CTS beads.

532.28 eV to 534.66 [43] and 532.38 eV after cobalt uptake, and to 531.30 and 532.52 eV after nickel adsorption. The peaks at 531.12, 534.66, and 531.30 eV and 532.28, 532.38, and 532.52 eV were assigned to C=O and –OH, respectively. Thus, it was confirmed that C=O and –OH groups acted as the main sorption sites by transferring charges to nickel ions or cobalt ions [33].

The result of Fig. 12 combined with those of Fig. 13 demonstrated that the amine groups on the biosorbent were protected by the template ions of nickel before cross-linking with ECH, thereby providing the primary binding sites for

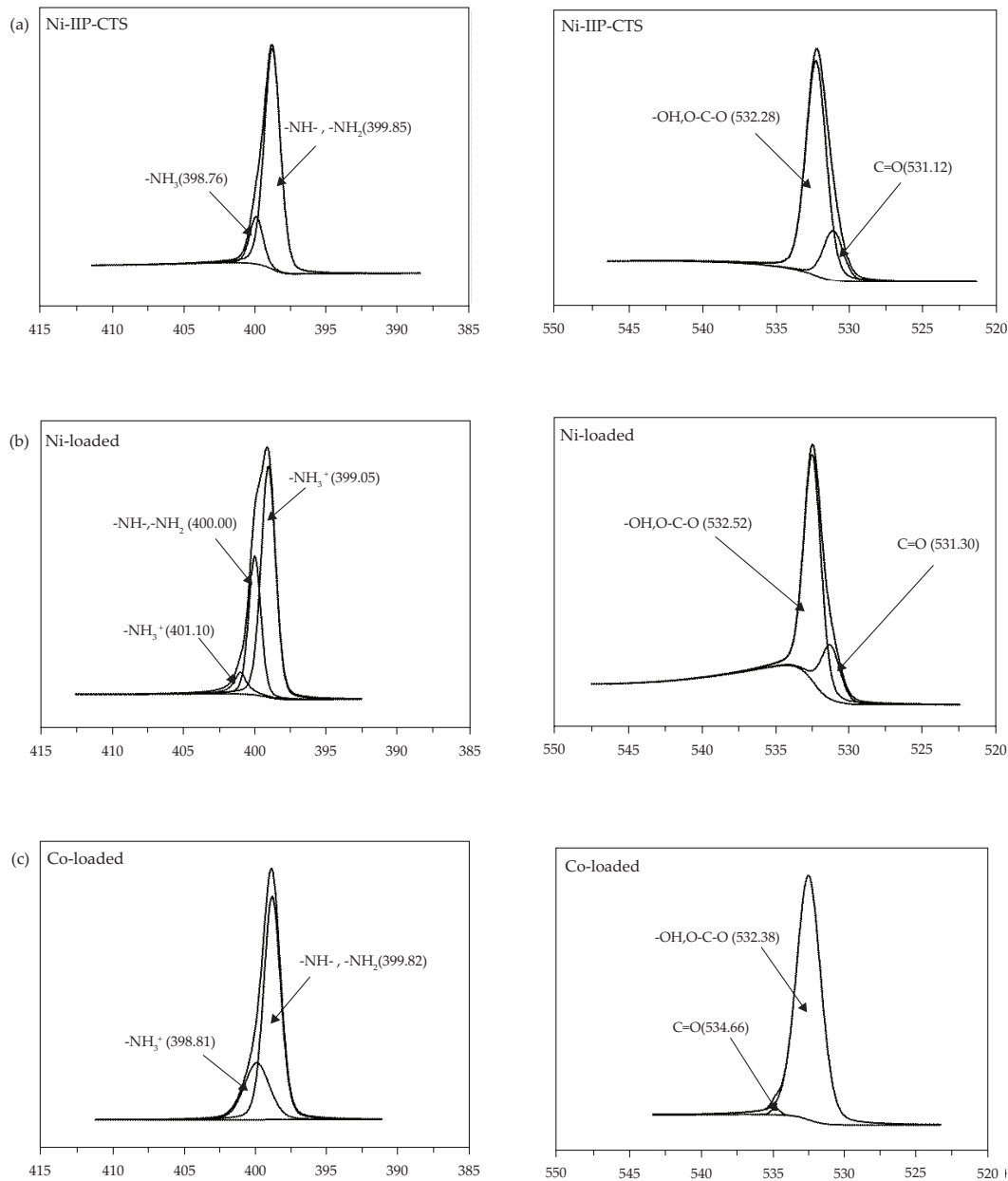


Fig. 13. XPS spectra of N 1s and O 1s element spectra of (a) Ni-IIP-CTS beads, (b) nickel-loaded Ni-IIP-CTS beads, (c) cobalt-loaded Ni-IIP-CTS beads.

the high selective adsorption of nickel. O-Containing groups displayed a similar affinity for nickel and cobalt, and therefore might instigate competitive adsorption between nickel and cobalt on Ni-IIP-CTS.

3.6.3. Mechanism of metal ion displacement

The results in Fig. 10 clearly demonstrated that early adsorbed cobalt ions on Ni-IIP-CTS were displaced by later adsorbed nickel ions in the adsorption process and the early adsorbed nickel ions were barely displaced by

later adsorbed cobalt ions. This phenomenon seems like an ion-exchange process in which a cobalt ion (or nickel ions) on Ni-IIP-CTS was exchanged by a nickel ion (or cobalt ions) to be adsorbed from the solution. Based on the study of Liu, et al. [44], the process was however different from that in a conventional ion-exchange process due to lacking net electric repulsion in a conventional ions exchange process such as $\text{R}^- - \text{Na}^+ + \text{Cu}^{2+} \rightarrow \text{R}^- - \text{Cu}^{2+} + \text{Na}^+$ (where R- denotes the whole resin base except the exchangeable ion, such as $\text{R}' - \text{COO}^-$, $\text{R}' - \text{SO}_3^-$). The release and adsorption of metal ion on the biosorbent in aqueous solution occurred simultaneously

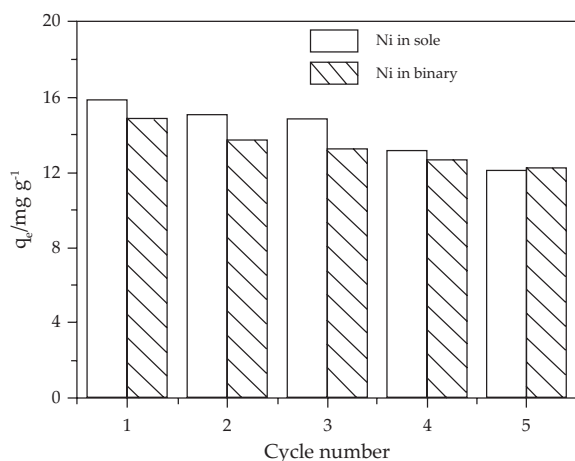


Fig. 14. Repeated adsorption of Ni²⁺ by Ni-IIP-CTS in sole and binary system.

and instantaneously until reaching adsorption equilibrium. It had been speculated that the displacement of cobalt ions by nickel was through an adjacent attachment and adjacent mechanism [44]. Nickel ions could be adsorbed to the adjacent adsorption sites due to high affinity to biosorbent and the release of cobalt ions. The adjacently adsorbed nickel ions could then dislodge the adsorbed cobalt ions from biosorbent and released it into solution. However, in other case studied, the amount of cobalt ions adsorbed on Ni-loaded biosorbent was near to be equal that the nickel ions released from the Ni-loaded biosorbent. Moreover, the cobalt ions showed lower affinity than nickel ions to biosorbent based on the laboratorial data and Irving-Williams order [45]. So the reason for cobalt-adsorbed on the Ni-loaded chitosan maybe that some metal adsorption sites of Ni-loaded adsorbent were in vacant state instantly after adsorbed nickel ions being released from the adsorption site of biosorbent and few vacant sites of Ni-loaded biosorbent, especially physical adsorption site, adsorbed cobalt ions adjacently. Further study in those aspects will have to be carried out to confirm such a speculation in the future.

3.7. Regeneration of Ni-IIP-CTS

For potential practical application, it is important to investigate the possibility of adsorbing the metal ions adsorbed on Ni-IIP-CTS. Five cycles of adsorption/desorption were carried out for nickel ions on Ni-IIP-CTS. EDTA solution (0.05 M) was used as an eluent. From Fig. 14, it can be seen the adsorption capacities of nickel ions were about 17.5% loss in pure nickel ions solution and about 19% loss in binary system after successive cycles up to 5 times, respectively. This indicated that Ni-IIP-CTS had good durability and efficiency for repeated use.

4. Conclusions

The selective biosorption of nickel on Ni-IIP-CTS biosorbent from a cobalt-and-nickel-containing solution was examined. The results showed that the selective adsorption of nickel was dependent on the solution pH, initial metal

ions concentration ratio, and contact time. The adsorption process was better described by the pseudo-second-order and Langmuir monolayer adsorption models regardless of the presence of interferent cobalt ions. Furthermore, previously adsorbed cobalt ions could be displaced upon subsequent adsorption of nickel ions in solution. The FTIR and XPS results revealed that the selective adsorption mechanisms could mainly involve chelation between N-containing groups and nickel ions, whereas the competitive adsorption mechanisms could involve chelation between the nickel or cobalt ions and O-containing groups. The K_d of nickel was higher than that of cobalt, thereby indicating the preferential adsorption of nickel on Ni-IIP-CTS. Five cycle runs indicated Ni-IIP-CTS had good durability and efficiency for repeated use. In summary, the present findings demonstrate the potential of Ni-IIP-CTS as an effective biosorbent for the separation of nickel and cobalt from leaching liquid and industry wastewater.

Acknowledgments

This project is supported by the National Natural Science Foundation of China (NSFC-51374150 and NSFC-51304140) and Science and Technology Plan Projects of Sichuan Province, China (Grant No. 2014SZ0146 and 2015HH0067).

References

- [1] C.Y. Cheng, M.D. Urbani, M.G. Davies, Y. Pranolo, Z. Zhu, Recovery of nickel and cobalt from leach solutions of nickel laterites using a synergistic system consisting of Versatic 10 and Acorga CLX 50, *Miner. Eng.*, 77 (2015) 17–24.
- [2] C. Chou, C. Hsieh, B. Chen, Hydrogen generation from catalytic hydrolysis of sodium borohydride using bimetallic Ni–Co nanoparticles on reduced graphene oxide as catalysts, *Energy*, 90 (2015) 1973–1982.
- [3] M.A. Rabah, F.E. Farghaly, M.A. Abd-El Motaleb, Recovery of nickel, cobalt and some salts from spent Ni-MH batteries, *Waste Manag.*, 28 (2008) 1159–1167.
- [4] Y. Shen, W. Xue, W. Niu, Recovery of Co(II) and Ni(II) from hydrochloric acid solution of alloy scrap, *Trans. Nonferrous Met. Soc. China*, 18 (2008) 1262–1268.
- [5] P. Hadi, J. Barford, G. McKay, Synergistic effect in the simultaneous removal of binary cobalt–nickel heavy metals from effluents by a novel e-waste-derived material, *Chem. Eng., J* 228 (2013) 140–146.
- [6] A. Fernandes, J.C. Afonso, A.J.B. Dutra, Separation of nickel(II), cobalt(II) and lanthanides from spent Ni-MH batteries by hydrochloric acid leaching, solvent extraction and precipitation, *Hydrometallurgy*, 133 (2013) 37–43.
- [7] Z. Zainol, M.J. Nicol, Comparative study of chelating ion exchange resins for the recovery of nickel and cobalt from laterite leach tailings, *Hydrometallurgy*, 96 (2009) 283–287.
- [8] M. Hutton-Ashkenny, D. Ibana, K.R. Barnard, Reagent selection for recovery of nickel and cobalt from nitric acid nickel laterite leach solutions by solvent extraction, *Miner. Eng.*, 77 (2015) 42–51.
- [9] R.A. Kumbasar, Selective extraction and concentration of cobalt from acidic leach solution containing cobalt and nickel through emulsion liquid membrane using PC-88A as extractant, *Sep. Purif. Technol.*, 64 (2009) 273–279.
- [10] M.A. Hashim, S. Mukhopadhyay, J.N. Sahu, B. Sengupta, Remediation technologies for heavy metal contaminated ground water, *J. Environ. Manage.*, 92 (2011) 2355–2388.
- [11] M. Monier, D.M. Ayad, Y. Wei, A.A. Sarhan, Adsorption of Cu(II), Co(II), and Ni(II) ions by modified magnetic chitosan chelating resin, *J. Hazard. Mater.*, 177 (2010) 962–970.

- [12] A. Chen, S. Liu, C. Chen, C. Chen, Comparative adsorption of Cu(II), Zn(II), and Pb(II) ions in aqueous solution on the cross-linked chitosan with epichlorohydrin, *J. Hazard. Mater.*, 154 (2008) 184–191.
- [13] A.M. Yousif, O.F. Zaid, I.A. Ibrahim, Fast and selective adsorption of As(V) on prepared modified cellulose containing Cu(II) moieties, *Arab J. Chem.* (2015).
- [14] E. Guibal, Interactions of metal ions with chitosan-based sorbents: a review, *Sep. Purif. Technol.*, 38 (2004) 43–74.
- [15] A.J. Varma, S.V. Deshpande, J.F. Kennedy, Metal complexation by chitosan and its derivatives: a review, *Carbohydr. Polym.*, 55 (2004) 77–93.
- [16] J. Wang, C. Chen, Chitosan-based biosorbents: modification and application for biosorption of heavy metals and radionuclides, *Bioresour. Technol.*, 160 (2014) 129–141.
- [17] Y. Liu, T. Liao, Z. He, T. Li, H. Wang, X. Hu, Y. Guo, Y. He, Biosorption of copper(II) from aqueous solution by *Bacillus subtilis* cells immobilized into chitosan beads, *Trans. Nonferrous. Met. Soc. China*, 23 (2013) 1804–1814.
- [18] A. Chen, C. Yang, C. Chen, C. Chen, C. Chen, The chemically crosslinked metal-complexed chitosans for comparative adsorptions of Cu(II), Zn(II), Ni(II) and Pb(II) ions in aqueous medium, *J. Hazard. Mater.*, 163 (2009) 1068–1075.
- [19] W.S. Ngah, S. Fatinathan, Adsorption characterization of Pb(II) and Cu(II) ions onto chitosan-tripolyphosphate beads: Kinetic, equilibrium and thermodynamic studies, *J. Environ. Manage.*, 91 (2010) 958–969.
- [20] H. Nishide, J. Deguchi, E. Tsuchida, Selective adsorption of metal-ions on crosslinked poly(vinylpyridine) resin prepared with a metal-ions as a template, *Chem. Lett.*, (1976) 169–174.
- [21] M. Monier, D.A. Abdel-Latif, Synthesis and characterization of ion-imprinted resin based on carboxymethyl cellulose for selective removal of UO_2^{2+} , *Carbohydr. Polym.*, 97 (2013) 743–752.
- [22] J. Wang, Z. Li, Enhanced selective removal of Cu(II) from aqueous solution by novel polyethylenimine-functionalized ion imprinted hydrogel: Behaviors and mechanisms, *J. Hazard. Mater.*, 300 (2015) 18–28.
- [23] H.R. Rajabi, S. Razmpour, Synthesis, characterization and application of ion imprinted polymeric nanobeads for highly selective preconcentration and spectrophotometric determination of Ni^{2+} ion in water samples, *Spectrochim. Acta A Mol. Biomol. Spectrosc.*, 153 (2016) 45–52.
- [24] M. Roushani, T.M. Beygi, Z. Saedi, Synthesis and application of ion-imprinted polymer for extraction and pre-concentration of iron ions in environmental water and food samples, *Spectrochim. Acta A Mol. Biomol. Spectrosc.*, 153 (2016) 637–644.
- [25] Y. Ren, M. Zhang, D. Zhao, Synthesis and properties of magnetic Cu(II) ion imprinted composite adsorbent for selective removal of copper, *Desalination*, 228 (2008) 135–149.
- [26] P.A. Nishad, A. Bhaskarapillai, S. Velmurugan, S.V. Narasimhan, Cobalt (II) imprinted chitosan for selective removal of cobalt during nuclear reactor decontamination, *Carbohydr. Polym.*, 87 (2012) 2690–2696.
- [27] M. Hossein Beyki, F. Shemirani, M. Shirkhodaie, Aqueous Co(II) adsorption using 8-hydroxyquinoline anchored γ -Fe $2O_3$ @chitosan with Co(II) as imprinted ions, *Int. J. Biol. Macromol.*, 87 (2016) 375–384.
- [28] M. Zhang, R. Helleur, Y. Zhang, Ion-imprinted chitosan gel beads for selective adsorption of Ag(+) from aqueous solutions, *Carbohydr. Polym.*, 130 (2015) 206–212.
- [29] L. Zhang, L. Zhong, S. Yang, D. Liu, Y. Wang, S. Wang, X. Han, X. Zhang, Adsorption of Ni(II) ion on Ni(II) ion-imprinted magnetic chitosan/poly(vinyl alcohol) composite, *Colloid Polym. Sci.*, 293 (2015) 2497–2506.
- [30] L. Zhou, C. Shang, Z. Liu, G. Huang, A.A. Adesina, Selective adsorption of uranium(VI) from aqueous solutions using the ion-imprinted magnetic chitosan resins, *J. Colloid. Interface Sci.*, 366 (2012) 165–172.
- [31] M. Monier, D.A. Abdel-Latif, Y.G. Abou El-Reash, Ion-imprinted modified chitosan resin for selective removal of Pd(II) ions, *J. Colloid Interface Sci.*, 469 (2016) 344–354.
- [32] N. Li, R. Bai, Copper adsorption on chitosan–cellulose hydrogel beads: behaviors and mechanisms, *Sep. Purif. Technol.*, 42 (2005) 237–247.
- [33] Y. Lin, G. Fryxell, H. Wu, Mark Engelhard selective sorption of cesium use self assembled monolayer on mesoporous supports, *Environ. Sci. Technol.*, 35 (2001) 3962–3966.
- [34] R. Juang, H. Shao, Effect of pH on Competitive Adsorption of Cu(II), Ni(II), and Zn(II) from Water onto Chitosan Beads, *Adsorpt*, 8 (2002) 71–78.
- [35] F. Yang, H. Liu, J. Qu, J.P. Chen, Preparation and characterization of chitosan encapsulated *Sargassum* sp. biosorbent for nickel ions sorption, *Bioresour. Technol.*, 102 (2011) 2821–2828.
- [36] M. Fouladgar, M. Beheshti, H. Sabzyan, Single and binary adsorption of nickel and copper from aqueous solutions by γ -alumina nanoparticles: Equilibrium and kinetic modeling, *J. Molecular. Liquids.*, 211 (2015) 1060–1073.
- [37] L. Mangaleswaran, A. Thirulogachandar, V. Rajasekar, C. Muthukumar, K. Rasappan, Batch and fixed bed column studies on nickel (II) adsorption from aqueous solution by treated polyurethane foam, *J. Taiwan. Inst. Chem. Eng.*, 55 (2015) 112–118.
- [38] B. Li, F. Liu, J. Wang, C. Ling, L. Li, P. Hou, A. Li, Z. Bai, Efficient separation and high selectivity for nickel from cobalt-solution by a novel chelating resin: Batch, column and competition investigation, *Chem. Eng. J.*, 195–196 (2012) 31–39.
- [39] S.N.d.C. Ramos, A.L.P. Xavier, F.S. Teodoro, M.M.C. Elias, F.J. Gonçalves, L.F. Gil, R.P. de Freitas, L.V.A. Gurgel, Modeling mono- and multi-component adsorption of cobalt(II), copper(II), and nickel(II) metal ions from aqueous solution onto a new carboxylated sugarcane bagasse. Part I: Batch adsorption study, *Ind. Crop. Pro.*, 74 (2015) 357–371.
- [40] A. Bhaskarapillai, S. Chandra, N.V. Sevilimedu, B. Sellergren, Theoretical investigations of the experimentally observed selectivity of a cobalt imprinted polymer, *Biosens. Bioelectron.*, 25 (2009) 558–562.
- [41] H. Su, J. Li, T. Tan, Adsorption mechanism for imprinted ion (Ni^{2+}) of the surface molecular imprinting adsorbent (SMIA), *Biochem. Eng. J.* 39 (2008) 503–509.
- [42] C. Liu, R. Bai, L. Hong, Diethylenetriamine-grafted poly(glycidyl methacrylate) adsorbent for effective copper ion adsorption, *J. Colloid Interface Sci.*, 303 (2006) 99–108.
- [43] D.T. Clark, HR, Applications of ESCA to polymer chemistry. 17. systematic investigation of core levels of simple homopolymers, *J. Polym. Sci., Part A: Polym. Chem.*, 16 (1978) 791–820.
- [44] C. Liu, R. Bai, Q. San Ly, Selective removal of copper and lead ions by diethylenetriamine-functionalized adsorbent: behaviors and mechanisms, *Water Res.*, 42 (2008) 1511–1522.
- [45] H. Strelko, Characterization and metal sorptive properties of oxidized active carbon, *J. Colloid Interface Sci.*, 250 (2002) 213–220.